Climate scenarios of sea level rise for the northeast Atlantic Ocean: a study including the effects of ocean dynamics and gravity changes induced by ice melt

Caroline A. Katsman, Wilco Hazeleger, Sybren S. Drijfhout, Geert Jan van Oldenborgh and Gerrit J. H. Burgers
*Royal Netherlands Meteorological Institute (KNMI), Global Climate Division, De Bilt, Netherlands**

revised version of December 21, 2007

Abstract.

Here we present a set of regional climate scenarios of sea level rise for the northeast Atlantic Ocean. In this study, the latest observations and results obtained with state-of-the-art climate models are combined. In addition, regional effects due to ocean dynamics and changes in the Earth's gravity field induced by melting of land-based ice masses have been taken into account. The climate scenarios are constructed for the target years 2050 and 2100, for both a moderate and a large rise in global mean atmospheric temperature (2° C and 4° C in 2100 respectively). The climate scenarios contain contributions from changes in ocean density (global thermal expansion and local steric changes related to changing ocean dynamics) and changes in ocean mass (melting of mountain glaciers and ice caps, changes in the Greenland and Antarctic ice sheets, and (minor) terrestrial water-storage contributions). All major components depend on the global temperature rise achieved in the target periods considered. The resulting set of climate scenarios represents our best estimate of twenty-first century sea level rise in the northeast Atlantic Ocean, given the current understanding of the various contributions. For 2100, they yield a local rise of 30 to 50 centimeter and 40 to 80 centimeter for the moderate and large rise in global mean atmospheric temperature, respectively.

Keywords: climate scenarios, local sea level rise

1. Introduction

In this paper, we present a new set of climate scenarios of sea level rise for the northeast Atlantic Ocean which can be used by stakeholders, such as government agencies responsible for coastal management. In constructing this new set, the latest observations and modeling results have been combined, similar to the approach used by Meehl et al. (2007a) to estimate global sea level rise. In addition, regional effects have been incorporated for both ocean and land ice contributions, in the form of local changes in ocean density associated with ocean dynamics

* Corresponding author: dr. C. A. Katsman, KNMI, Global Climate Division, PO Box 201, 3730 AE De Bilt, Netherlands, katsman@knmi.nl

© 2007 *Kluwer Academic Publishers. Printed in the Netherlands.*

and the effects of changes in the Earth's gravity field resulting from the redistribution of mass due to melting of land-based ice masses.

The Royal Netherlands Meteorological Institute (KNMI) first presented a set of three climate scenarios (low, central and high) in 2000, for the target years 2050 and 2100. The underlying scientific basis of these climate scenarios was the projection for global mean sea level rise discussed in the second IPCC Assessment Report (Houghton et al., 1995). To account for differences between local sea level rise in the area of interest and global sea level rise, another 10 cm (one to two times the standard deviation of the regional variations displayed by climate models at that time; Houghton et al. 1995), was added to the high climate scenario only.

Recently, KNMI researchers extended that simple methodology (van den Hurk et al., 2006). To construct a set of new climate scenarios, results from a suite of state-of-the-art climate models and recent observations were combined in a consistent manner. The contribution of the thermal expansion of the ocean was analyzed focusing on the northeast Atlantic Ocean to include the effects of changes in the regional ocean circulation on sea level. In this paper, the methodology is further refined by including the effects that the redistribution of mass associated with the melting of land-based ice masses has on the Earth's gravity field (Woodward, 1888) and hence on local sea level. This in contrast to the assumption of a eustatic rise resulting from the reduction of land-based ice masses applied in van den Hurk et al. (2006).

Section 2 describes the general methodology adopted by KNMI in developing the climate scenarios presented in 2006, as well as aspects specific for the climate scenarios of sea level rise. The various contributions to sea level rise that are taken into account are discussed in Sections 3, 4 and 5. The final climate scenarios are presented in Section 6, along with a discussion (Section 7).

2. The KNMI'06 climate scenarios

For atmospheric parameters, the KNMI'06 climate scenarios were constructed for the target year 2050 relative to 1990 using two steering parameters (for details see van den Hurk et al., 2006): the rise in global atmospheric temperature since 1990 (ΔT_{atm}) projected by large-scale climate models (Atmosphere-Ocean General Circulation Models or AOGCMs) and the variation in the atmospheric circulation over Western Europe simulated by AOGCMs. The latter parameter was found to have a large influence on seasonal mean precipitation in the region of interest (van Ulden and van Oldenborgh, 2006; Lenderink

et al., 2007). Using these two steering parameters, four different climate scenarios were defined, representing the impacts of moderate or large atmospheric warming, with either an unchanged or a changed circulation over Europe.

Although it can be expected that changes in the local atmospheric circulation affect the mean water level in marginal seas such as the North Sea, the current generation of AOGCMs does not have sufficient resolution to resolve this. Hence, for sea level rise, we were forced to omit the variation in the atmospheric circulation over Western Europe as a steering parameter, and climate scenarios were defined for a moderate and large rise in global atmospheric temperature only. On the other hand, because of the obvious needs for long-term planning with regard to coastal management, climate scenarios of sea level rise were constructed for the target years 2050 and 2100. In this way, a set of four climate scenarios of sea level rise was defined (van den Hurk et al., 2006).

The Intergovernmental Panel on Climate Change (IPCC) presents climate change projections grouped by specific emission scenarios in their assessment reports (Solomon et al., 2007a; Houghton et al., 2001). These emission scenarios represent storylines of economic, social and technical development. The KNMI'06 climate scenarios are not distinguished based on these storylines, because the ranges of global atmospheric temperature rise of the different storylines overlap considerably halfway into the twenty-first century. This also holds for the projected changes in sea level (Solomon et al., 2007b, their Table SPM-1). At present, uncertainties in the projections for global mean atmospheric temperature and global mean sea level are mainly due to model uncertainties, reflected by a wide range in results from AOGCM simulations with a common emission scenario (see for example Meehl et al., 2007a, Figure 10.31). Uncertainty about emissions of greenhouse gases plays a smaller role. In light of this large model uncertainty, it is advantageous to have a large model ensemble for the analysis that follows. As in van den Hurk et al. (2006), we therefore express the climate scenarios grouped by global mean atmospheric temperature rise rather than by emission scenario.

2.1. Definition of steering parameters

The values for global mean atmospheric temperature rise that define the climate scenarios (van den Hurk et al., 2006) are selected based on an analysis of AOGCM simulations forced by the A1B, B1 and A2 emission scenarios performed in preparation of the Fourth IPCC Assessment Report (Solomon et al., 2007a). These simulations have been

made available to the scientific community in the form of the World Climate Research Programme's (WCRP's) Coupled Model Intercomparison Project phase 3 (CMIP3) multi-model dataset (Meehl et al., 2007b). These AOGCMs simulate values of global mean atmospheric temperature rise between 1990 and 2050 of $\Delta T_{atm} = 1.1\ ^\circ$ C to $2.0\ ^\circ$ C, and of $\Delta T_{atm} = 1.6\ ^\circ$ C to $4.3\ ^\circ$ C for 2100 (van den Hurk et al., 2006). Hence, atmospheric temperature rises of $+1\ ^\circ$ C and $+2\ ^\circ$ C are used for 2050, and values of $+2\ ^\circ$ C and $+4\ ^\circ$ C for 2100. These values roughly correspond to the 10% and 90% points of the probability distribution function of the temperature rise (see Figure 1 for the distribution for target year 2100).

It should be noted, however, that a higher temperature increase for 2100 could eventually be justified, since the AOGCM simulations in the CMIP3 database do not account for the full uncertainty of the climate system. Feedbacks that are known to influence the climate system on century-long time scales, such as carbon cycle feedbacks and vegetation feedbacks, are not or only very crudely represented in these AOGCMs (Friedlingstein et al., 2006). On one hand, perturbed physics ensembles indicate higher climate sensitivities than displayed by these state-of-the-art AOGCMs (Stainforth et al., 2005). On the other hand, analyses of instrumental and proxy records indicate that the climate sensitivity displayed in these AOGCMs is realistic (Hegerl et al., 2006). Sudden changes in the climate system induced by rapid disintegration of ice sheets (Oppenheimer, 1998) or a complete collapse of the thermohaline circulation (Vellinga and Wood, 2002) are not included in this ensemble of simulations either.

2.2. Constructing climate scenarios of sea level rise

Global mean sea level may change because of a change in the amount of mass in the ocean, or by a change in the average density of the ocean (steric changes)[1]. Global mean changes in ocean density are dominated by the thermal expansion of ocean water, referred to as the thermosteric contribution. Halosteric changes induced by salinity variations may be important locally (see below) but play only a minor role in the global mean (Bindoff et al., 2007).

Local changes in sea level may differ from the global mean due to variations in surface winds and ocean currents, spatial variations in ocean heat uptake (Levitus et al., 2000), salinity variations (Boyer et al., 2005) and changes in the Earth's gravity field associated with

[1] Changes in the ocean basin volume due to sedimentation and tectonic movements are neglected here

the redistribution of mass resulting from the release of melt water from land-based ice masses (Woodward, 1888; Mitrovica et al., 2001).

To construct climate scenarios of sea level rise for the northeast Atlantic Ocean, contributions from various sources are considered here. For the period 1990-2005, observations of local sea level rise are used for all climate scenarios (Section 3). From 2005 onwards, changes in ocean density (global mean thermal expansion and local steric changes, Section 4) and changes in ocean mass (melting of mountain glaciers and ice caps, changes in the Greenland and Antarctic ice sheets, and (minor) terrestrial water-storage contributions, Section 5) are considered separately. Local sea level changes from the ocean mass sources are based on estimates for eustatic changes and the effects of the associated gravity changes on local sea level.

All major components of the sea level rise estimates depend on the global atmospheric temperature rise ΔT_{atm} achieved in the target periods considered. Hereby, it is taken into account that part of this atmospheric temperature rise is already achieved in the period 1990-2005. Currently, the global mean atmospheric temperature is about 0.3 $^{\circ}$ C higher than in 1990 (derived from low-pass filtered HadCRUT3 global temperature index, Brohan et al., 2006; Rayner et al., 2006; see www.climexp.knmi.nl).

3. Observed total sea level rise 1990-2005

For all climate scenarios, sea level rise over the period 1990-2005 is defined based on recent observations. The global mean rate of sea level rise over the twentieth century deduced from tide gauges is 1.7 ± 0.3 mm/year (Holgate and Woodworth, 2004; Church and White, 2006). Solomon et al. (2007b) report a global mean rise of 1.8 ± 0.5 mm/year for the period 1961-2003, and an accelerated rise revealed by satellite radar altimetry of 3.1 ± 0.7 mm/year for the period 1993-2003.

Along the coast of the Netherlands, such an acceleration has not been observed over the last decades. There, sea level rose at a steady rate of about 2.5 ± 0.6 mm/yr (data by RWS National Institute for Coastal and Marine Management, the Netherlands). This observed local rate of sea level rise is applied in the climate scenarios, yielding a contribution of 4 ± 1 cm for the period 1990-2005 (Table IV).

4. Changes in ocean density

The contribution of steric sea level changes is estimated based on an analysis of sea level data for the twenty-first century from AOGCM simulations in the CMIP3 database (Meehl et al., 2007b). Some model results were discarded after a quality check, because of obvious deficiencies in the data (UKMO HadGem1, IPSL CM4). The dataset that is used for the analysis consists of 41 simulations forced by the A1B, the A2 or the B1 emission scenario (Solomon et al., 2007a), obtained with 13 different AOGCMs (Table I).

Three variables of interest were retrieved: timeseries of global mean thermosteric sea level rise, fields of local sea level changes, and fields of atmospheric temperature rise. Only from three AOGCMs, both types of sea level variables were available (Table I). Except for the isopycnic model $BCCR-BCM2.0$, the global mean of the reported fields of local steric changes is zero by definition, because sea level is defined to relate to the instantaneous volume of the ocean. This is a natural definition for models that are volume conserving rather than mass conserving. Actual sea level changes need to be calculated based on the (changes in the) density fields. The timeseries of global mean thermosteric sea level rise reported by the modeling groups are the results of such a procedure based on the temperature fields only. Timeseries of global mean halosteric sea level rise are not available from the CMIP3 database. The contribution for the local steric change was therefore split into an estimate for global mean thermosteric sea level rise (TS_G, obtained from the reported time series of global mean thermosteric sea level rise) and for the difference in steric change between the North Atlantic Ocean and the global mean (THS_L, obtained from the fields of local sea level changes). The model ensemble on which these contributions are based consists of 6 members for TS_G (10 members for THS_L).

The fields for local steric sea level change are interpreted as the sum of the local thermosteric and halosteric sea level rise. Except for the GISS models (Lucarini and Russell, 2002; Schmidt et al., 2004), the land ice distribution is kept fixed in all analyzed AOGCMs, and there is no contribution from changes in ocean mass in the local sea level data. The local data from the GISS models are discarded from the analysis because the land ice contribution they contain can not be separated from the steric signal. Furthermore, it is assumed that the modeled contribution of changes in the terrestrial water storage is negligible (see Section 5.4 for a separate treatment of this contribution).

A time series over the region [25° W,10° E] × [40° N, 65° N] was constructed from the fields of steric sea level change to obtain an estimate of the additional steric sea level rise THS_L in the northeast Atlantic

Ocean. The monthly time series for TS_G, TSH_L and atmospheric temperature rise ΔT_{atm} were converted to year-averaged timeseries and smoothed using a five-year running mean.

4.1. Global mean thermosteric sea level rise (TS_G)

Projections for ΔT_{atm} and TS_G for the twenty-first century were presented by Solomon et al. (2007a). While ΔT_{atm} is expected to rise more or less linearly over the course of the century (Meehl et al., 2007a, Fig. 10.4), sea level responds slower and accelerates toward the end of the twenty-first century (Meehl et al., 2007a, Fig. 10.31). For the three emission scenarios considered here the reported ranges for global mean thermosteric sea level rise between 1980-1999 and 2090-2099 are 13-32 cm (A1B scenario), 14-35 cm (A2 scenario) and 10-24 cm (B1 scenario, from Table 10.7 of Meehl et al., 2007a).

In a study on modeled thermosteric sea level changes in the twentieth century (Urrego Blanco and Katsman, document in preparation) it was found that AOGCM results for TS_G from the CMIP3 database may be contaminated by model drift. In the accompanying pre-industrial control runs, in which the atmospheric forcing is kept constant and hence global mean thermosteric sea level is expected to reach a steady state. However, many of the AOGCMs display a fairly linear drift of up to ten centimeters per century. This suggests that these models were not spun up long enough to reach equilibrium in the (deep) ocean. This was also noted by Gregory et al. (2001) with regard to simulations prepared for Houghton et al. (2001). Following Gregory et al. (2001) and Urrego Blanco and Katsman (document in preparation), it is assumed that the SRES scenario runs analyzed here contain a similar drift as the accompanying pre-industrial control runs, in addition to the signal of ocean expansion we want to quantify as the contribution TS_G. Therefore, all timeseries for TS_G were corrected for model drift by subtracting the linear trend in the timeseries of the accompanying pre-industrial control run. The effects of this procedure are illustrated in Figure 2a, which shows the original data against the drift-corrected data for TS_G, for the year 2100 relative to 2005. The data for atmospheric temperature rise were corrected in the same way for completeness, although the drift in this variable is much smaller (Fig. 2b). Although in individual models the drift can be substantial, this drift-correction procedure introduces differences of only a few centimeters in the ensemble mean results for TS_G in comparison with the uncorrected results presented by van den Hurk et al. (2006).

In Figure 3, the simulated global mean thermosteric sea level rise (TS_G) in 2050 and 2100 (relative to 2005) is plotted against the sim-

ulated global mean temperature rise ΔT_{atm} since 1990 (ΔT_{atm} since 1990 is defined as ΔT_{atm} since 2005 + 0.27° C). For the end of the twenty-first century, the AOGCMs project $TS_G = 10-35$ cm. For 2050, $TS_G = \pm 5-10$ cm. The dependency of TS_G on the atmospheric temperature change is described by a linear fit through the data for each of the target years (solid lines in Figure 3). We assume an uncertainty that is independent of ΔT_{atm}, and define it as one standard deviation of the fit parameters at the central value of ΔT_{atm} for the two periods (dashed lines in Figure 3). Thus one can read from this figure the lower and upper estimates for TS_G at $\Delta T_{atm} = 1°$ C and 2° C in 2050 and at $\Delta T_{atm} = 2°$ C and 4° C in 2100 that are required to construct the climate scenarios. The results are given in Table II.

4.2. Additional steric sea level rise in the northeast Atlantic Ocean (THS_L)

To analyze the difference in steric sea level between the northeast Atlantic Ocean and the global mean, fields for local sea steric level change (interpreted as the sum of the local thermosteric and halosteric sea level rise) were obtained from the CMIP3 database (Meehl et al., 2007b). Except for the isopycnic model $BCCR-BCM2.0$, the global mean of these fields is zero by definition, because sea level is defined to relate to the instantaneous volume of the ocean. This is the natural definition for models that are volume conserving rather than mass conserving. Hence, these fields do not display a model drift, and need not be corrected. The results from the $BCCR-BCM2.0$ model are corrected for the slight linear drift of 1.2 cm/century in the pre-industrial control run.

Regionally, changes in thermosteric sea level rise can deviate substantially from the global mean value (Cazenave and Nerem, 2004; Solomon et al., 2007a). In many of the analyzed AOGCM simulations, sea level in the North Atlantic Ocean increases more than the global mean sea level (see Solomon et al., 2007a, Figure 10.32 for the difference between averages for 2080-2099 and 1980-1999 from 16 AOGCMs forced with the SRES A1B scenario).

Figure 4 shows the difference in steric sea level between the northeast Atlantic Ocean and the global mean value THS_L projected by the AOGCMs, but now as a function of atmospheric temperature rise ΔT_{atm}, for target years 2050 and 2100. The mean hardly displays a dependence on ΔT_{atm}. However, the scatter tends to increase with atmospheric temperature rise, and is asymmetric with respect to the mean: the uncertainty at the high end of the range is larger than at the low range. From Figure 4, two types of model behavior emerge. Either THS_L is close to zero regardless of ΔT_{atm}, or THS_L increases

sharply with rising atmospheric temperatures. The latter behavior reflects dynamical sea level changes associated with circulation changes that occur in a selection of the model simulations. In particular, the difference in steric sea level between the North Atlantic Ocean and the global mean is strongly related to the strength of the meridional overturning circulation (AMOC) in the basin. In state-of-the-art AOGCM simulations the AMOC weakens by about 25% (bandwidth 0-50%) over the course of the twenty-first century (see Solomon et al., 2007a, Figure 10.15, from Schmittner et al., 2005).

Figure 5 shows the local steric sea level rise THS_L against the maximum strength of the AMOC (note that only the models marked by an asterisk in Table I, for which the latter variable was available in the CMIP3 database, are plotted). In some of the simulations, the AMOC is significantly reduced, and THS_L is relatively large. When the strength of the AMOC hardly changes, THS_L appears close to zero. Such dynamic changes in sea level associated with AMOC changes were also discussed by Levermann et al. (2004) and van der Schrier et al. (2004).

To account for the asymmetric behavior resulting from possible changes in ocean dynamics displayed in Figures 4 and 5, the following procedure was used to estimate the contribution of local steric changes THS_L. We assume a linear dependence of THS_L and its uncertainty bands on ΔT_{atm}. This dependence is quantified by calculating the ratio between THS_L and ΔT_{atm} for all data points at five-year intervals (black dots in Figure 4). The slope of the solid line, from which the central value of the contribution is derived, is the median value of all the calculated ratios (0.8 cm/K). The slopes of the dashed lines, defining the upper and lower uncertainty bands of the contribution, respectively, are the 10% and 90% values of all the calculated ratios (-0.8 cm/K and +4.2 cm/K). The contribution for THS_L for the various climate scenarios is obtained by multiplying these slopes by the appropriate atmospheric temperature changes (Table II).

The contributions of global mean TS_G and additional local THS_L (Table II) are combined by adding the central values. The total uncertainty ranges are defined by adding their bandwidths quadratically. The final results are listed in Table IV.

5. Changes in ocean mass

Changes in ocean mass occur through melting of land-based ice masses and changes in terrestrial water-storage contributions (e.g., changes in ground water, lakes, rivers and snow pack, see Section 5.4; Houghton

et al., 2001). Melting of mountain glaciers and ice caps (Section 5.2) and shrinking of the Greenland and Antarctic ice sheets (Section 5.3) are the main ocean mass contributons to sea level rise.

5.1. Gravity changes induced by ice melt

When ice masses on land melt, the released fresh water is not distributed evenly over the oceans (Woodward, 1888; Mitrovica et al., 2001). Large land-based ice masses exert a gravitational pull on the surrounding ocean and hence sea level is relatively high in the vicinity if the ice mass (see schematic in Fig. 6). When the ice mass shrinks, that pull reduces, and sea level will actually drop over a distance up to about 20° (2200 km) from the ice sheet (area A in Fig. 6) rather than rise due to the added melt water (Farrell and Clark, 1976). Farther away from the land ice mass, up to a distance of about 60° (6700 km, area B), sea level does rise, but this rise is smaller than the rise that would result from equal distribution of the melt water (the eustatic sea level rise). At even greater distances the local sea level rise becomes larger than the eustatic rise (area C). As a result of these local gravity changes, a shrinking land ice mass yields a distinct pattern of local sea level rise referred to as its fingerprint (Farrell and Clark, 1976; Mitrovica et al., 2001). Fingerprints have been used to identify the origin of global melt water pulse 1A (Clark et al., 2002; Bassett et al., 2007).

Mitrovica et al. (2001) presented maps of the ratio of the local sea level rise (including effects of changes in gravitation) and the eustatic rise, assuming shrinking of the Antarctic ice sheet, Greenland ice sheet, and of a collection of the world's glaciers (Meier, 1984) respectively. The computed fingerprints show that western Europe lies in area B with regard to the Greenland ice sheet and the collection of glaciers, and in area C with regard to the Antarctic ice sheet.

In the KNMI'06 climate scenarios of sea level rise (van den Hurk et al., 2006), the effect of gravity changes was not taken into account. The contributions from land ice melt were all summed and assumed to be eustatic. Here, the impacts of gravitation changes are incorporated by multiplying the eustatic contributions from ice melt by the appropriate ratio of local sea level rise and eustatic rise in the northeast Atlantic Ocean given by Mitrovica et al. (2001, their Figure 1).

5.2. Mountain glaciers and ice caps

The response of mountain glaciers and ice caps outside Greenland and Antarctica to atmospheric warming is characterized by means of the sensitivity B_g of their mass balance to global temperature increase, expressed in mm/yr/K. The changes in melting behavior resulting

from changes in the shape of the glaciers during retreat are taken into account by assuming that B_g is proportional to ice area A, and that ice volume and ice area scale as $V_g \sim A^{\alpha}$ (Bahr et al., 1997; van de Wal and Wild, 2001). Although this scaling law was derived for individual glaciers in a steady state, we apply it here to the whole ensemble, as was suggested by Wigley and Raper (2005). The fact that most of the considered glaciers are not in a steady state but retreating may introduce errors of the order of 20% (Meehl et al., 2007a). A wide range of sensitivities B_g and volumes V_g is used in the calculations of the glacier contribution to cover such uncertainties.

The sensitivity of the mass balance B_g is assumed to change over time according to

$$B_g(t) = B_0 \frac{V_g(t)}{V_0}^{1/\alpha} \tag{1}$$

with B_0 and V_0 the present-day sensitivity and ice volume of the glaciers, respectively. The proportionality constant α=1.375 is taken from Bahr et al. (1997). At any given year y, the melt rate M_g is given by B_g times the difference ΔT between the global mean atmospheric temperature and the equilibrium temperature of the glaciers:

$$M_g(t) = B_g(t)\Delta T(t) = B_g(t)[\Delta T_{atm}\frac{y_t - y}{y_t - y_0} + \Delta T_{eq}] \tag{2}$$

with y_t the target year (2050 or 2100), y_0 the base year (2005) and ΔT_{atm} the global mean atmospheric temperature rise defined for a specific climate scenario. ΔT_{eq} is an off-set temperature representing the current difference between the global mean atmospheric temperature and the equilibrium temperature of the glaciers. The eustatic contribution of glacier melt for a given climate scenario is obtained by integrating Equation (2) from the base year y_0 to the target year y_t.

We assume a present-day temperature off-set of ΔT_{eq}=1° C over equilibrium for the glaciers (representing the global mean atmospheric temperature rise since pre-industrial times, see the discussion below), and define $B_0 = 0.8 \pm 0.2$ mm/yr/K. These parameter values correspond to observation-based estimates of the current contribution of mountain glaciers to sea level rise of 0.5 ± 0.2 mm/yr for the period 1960-2003 and 0.8 ± 0.2 mm/yr for the last decade (Kaser et al., 2006; Solomon et al., 2007b). Estimates of the total ice volume currently stored in mountain glaciers and ice caps outside Greenland and Antarctica range from 15 cm to 37 cm sea level rise equivalent (Ohmura, 2004; Dyurgerov and Meier, 2005; Lemke et al., 2007). For our calculations, we use $V_0 = 20$ cm as the central value and V_0=10 cm and V_0=40 cm as the upper and lower bounds, respectively.

Using these parameters, the melt rate M_g in Equation 2 increases over time to a final value between 0.6 mm/yr and 2.5 mm/yr in 2100 for the different climate scenarios. The eustatic contribution of the glaciers and ice caps for the four climate scenarios (listed in Table III) is obtained by integrating Equation 2 for the specified values of ΔT_{atm} over the appropriate period. Uncertainty bands are defined by adding uncertainties with regard to the range in B_g and the range in V_g quadratically.

The eustatic contribution between 2005 and 2100 estimated in this way ranges from 4 to 19 cm depending on the assumed temperature rise. The results of the calculation appear not very sensitive to the choice of the present-day temperature off-set ΔT_{eq}. Doubling it to 2° C yields an increase in the central estimates of 3 cm or less in 2100. The bandwidth increases by just 1 cm. A lower value for ΔT_{eq} of 0.5 ° C yields a reduction of the eustatic glacier contribution by less than 2 cm and a slight (< 1 cm) reduction of the bandwidth.

Meehl et al. (2007a) estimate the eustatic contribution of glaciers and ice caps at 7 to 16 cm. This range is slightly narrower than ours, but the central estimates from the two studies are very similar. The melt rate projected for the end of the century is somewhat smaller similar (0.5 to 1.9 mm/yr for the selected emission scenarios, see Table 10.7 in Meehl et al., 2007a). Gregory and Oerlemans (1998) and Raper and Braithwaite (2006) model glacier melt using a regional glacier model forced by AOGCM output. Their approaches are more sophisticated than ours, as they distinguish between melting behavior in summer and non-summer months (Gregory and Oerlemans, 1998) and allow glaciers to approach a new equilibrium as their environment warms (Raper and Braithwaite, 2006), for example. Gregory and Oerlemans (1998) arrive at an estimate of 13 cm eustatic sea level rise due to glacier melt in 2100, which is at the high end of our estimates for the moderate and warm climate scenario (Table III). Raper and Braithwaite (2006) start with a melt rate at the low end of the observed range (0.2 mm/year), so the numerical value that they obtain for eustatic sea level rise in 2100 (5 cm), is at the very low end of our estimates. It should be noted that this approach, as the ones adopted by Gregory and Oerlemans (1998) and Raper and Braithwaite (2006), assumes that glacier motion is unchanged as atmospheric temperatures rise. This may result in an underestimation of the contribution of mountain glaciers. In a recent assessment, Meier et al. (2007) project a eustatic contribution from glaciers by extrapolating observed accelerations in the rate of change of the mass balance over the past decade to the end of the century. Their estimated range of of 10 to 25 cm in 2100 is about 5 cm larger than ours.

To account for the effects of gravity changes induced by glacier melt, the eustatic contribution is multiplied by a factor 0.8, derived from the ratio between the local sea level rise and the eustatic rise along western Europe for the collection of glaciers presented in (Mitrovica et al., 2001, their Figure 1c). This only induces a change of a few centimeters to the contribution. The final local results applied in the climate scenarios are presented in Table IV.

5.3. Greenland and Antarctic ice sheets

At present it is unclear how the Greenland and Antarctic ice sheets will respond to atmospheric warming, as recent observations and modeling results disagree (see Solomon et al., 2007a, and the discussion below). As a consequence, large uncertainties are involved in the estimate of their contributions to sea level rise. As in van den Hurk et al. (2006), we base the eustatic contributions from the ice sheets on estimates of (i) the present-day melt rate M , (ii) the sensitivity of the mass balance of the ice sheets to global mean atmospheric temperature rise B and (iii) the impacts of relatively fast changes in the ice dynamics in response to large rises in atmospheric temperature expressed in the form of a maximum sensitivity of the mass balance B_{max}. The sensitivity of the mass balance of the ice sheets to global mean atmospheric temperature rise B is assumed constant here for simplicity, even though model simulations show that this may not be the case (Gregory and Huybrechts, 2006). To include the effects of gravitation changes on local sea level (Mitrovica et al., 2001), the two ice sheets are treated separately.

5.3.1. *Greenland ice sheet*

Estimates for the present-day sea level change due to the melting of the Greenland ice sheet, including the glaciers and small ice caps around its edges, have been obtained by remote sensing over the last few decades (see Shepherd and Wingham, 2007 and Lemke et al., 2007 for a review). Even though the Greenland ice sheet thickens at its center (Johannessen et al., 2005), the ice sheet as a whole loses mass. Lemke et al. (2007) report an equivalent rate of sea level rise due to mass loss of the Greenland ice sheet of $M_{GL} = 0.21\pm\ 0.07$ mm/yr for 1993-2003. Compared to the period 1961-2003 this implies an acceleration of the mass loss; the forty-year average being $M_{GL} = 0.05\pm\ 0.12$ mm/yr (Lemke et al., 2007). On the basis of these observational results we estimate that at present the shrinking of the Greenland ice sheet yields a eustatic sea level rise of $M_{GL} = 0.2\pm\ 0.1$ mm/yr. The high end of the range is the same as the central estimate presented by (Shepherd and Wingham, 2007) of a eustatic sea level rise of about 0.3 mm/yr, based

on a series of studies using satellite observations from various periods over the last two decades.

Measurements are too sparse, and time series too short to asses the sensitivity of the mass balance of the ice sheets to atmospheric temperature rise with confidence on the basis of observations. Model projections of the sensitivity of the mass balance of the Greenland ice sheet to global mean atmospheric temperature rise for the twenty-first century are highly uncertain (Huybrechts et al., 2004; Gregory and Huybrechts, 2006). For the Greenland ice sheet the net balance points to increased mass loss for rising temperatures. The estimate of the temperature dependence of the ice sheet mass balance B_{GL} from 18 coupled climate models forced with an AR4 emission scenario is $B_{GL} = 0.11 \pm 0.09$ mm/yr/K with respect to local temperature (Huybrechts et al., 2004; Gregory and Huybrechts, 2006). The polar amplification of temperature over Greenland is approximately a factor 1.6 (median value obtained from Huybrechts et al. 2004, Table 2). To construct the climate scenarios, we therefore use $B_{GL} = 0.2 \pm 0.15$ mm/yr/K with respect to global mean temperature changes.

Currently, observations predict a larger contribution to sea level rise than the models simulate for this period. Numerical ice sheet models are not yet able to represent ice dynamics that may be of importance for the behavior of the Greenland ice sheet (Meehl et al., 2007a), like accelerated ice flows caused by for example basal lubrication (Zwally et al., 2005), ice shelf removal (Joughin et al., 2004) or the ungrounding of ice fronts (Howat et al., 2005). Accelerated ice flow (Krabill et al., 2004; Rignot and Kanagaratnam, 2006) could dramatically increase the contribution to sea level rise, but quantitative projections over the course of this century are almost impossible to make. Climate simulations of the last interglacial period (130,000 years ago) by Otto-Bliesner et al. (2006) show that for climate conditions with a local temperature rise of +3° C compared to present-day climate, the Greenland ice sheet had melted to about half its current size (3.4 m sea level equivalent), but this melting process took about three thousand years. This yields an estimate for the mass balance sensitivity of $B_{GL,max} = 0.4$ mm/yr/K with respect to the local temperature. Ridley et al. (2005) simulated the behavior of the Greenland ice sheet in a high CO_2 climate. They assessed a mass loss that peaked at values exceeding 4 mm/yr (40% of the ice volume lost in six to seven centuries, see also Fig. 10.38 in Meehl et al., 2007a), in response to a global mean temperature rise of about 3° C, yielding $BGL, max = 1.3$ mm/yr/K. To incorporate the high end of these uncertainties in BGL, max in our climate scenarios, we define an upper bound of the sensitivity of the mass balance $B_{GL,max}$=1.3 mm/yr/K based on the model results of Ridley et al. (2005).

In the climate scenarios, the central value of the melt rate of the Greenland ice sheet to sea level rise $M_{GL,tot}$ is the sum of the present-day melt rate of $M_{GL} = 0.2\pm\ 0.1$ mm/yr and the estimate for the mass balance sensitivity ($B_{GL} = 0.2 \pm 0.15$ mm/yr/K) times the atmospheric temperature rise averaged over the target period considered (2005-2050 or 2005-2100). The lower bound of the contribution is defined by adding the uncertainties in M_{GL} and $B_{GL}\ \Delta T_{atm}$ quadratically. The upper bound is calculated by adding the uncertainties in M_{GL} and $(B_{GL,max} - B_{GL})\ \Delta T_{atm}$ quadratically. Table III lists the eustatic sea level rise contribution of melting of the Greenland ice sheet. These eustatic contributions are multiplied by a factor 0.25 (obtained from Fig. 1b of Mitrovica et al., 2001), to account for the effects of gravity changes on local sea level in the area of interest. The local contribution induced by melt of the Greenland ice sheet is listed in Table IV for all climate scenarios.

5.3.2. *Antarctic ice sheet*

Satellite-based estimates for the mass change of the Antarctic ice sheet, including glaciers and small ice caps around its edges, vary widely. In their review, Shepherd and Wingham (2007) conclude that the East Antarctic Ice Sheet is gaining mass at a rate of about 25 Gt/year, while the West Antarctic Ice Sheet is losing mass at a rate of about 50 Gt/year (note that both numbers have large uncertainties). In particular, glaciers draining into the Amundsen Sea displayed large perturbations recently. Shepherd and Wingham (2007) report a central estimate for the net mass loss of 25 Gt/yr for the Antarctic ice sheet, from a range of -139 Gt/yr to + 42 Gt/yr in central estimates from various studies. This mass loss is equivalent to a eustatic sea level rise of $M_{AA} = 0.07$ mm/yr (range is 0.4 to -0.12 mm/yr). Lemke et al. (2007) report a eustatic sea level rise of $M_{AA} = 0.2\pm\ 0.35$ mm/yr due to changes in the Antarctic ice sheet over the period 1993-2003, a similar range as in Shepherd and Wingham (2007). For the climate scenarios, we therefore use the Lemke et al. (2007) estimate for the present-day melt rate of the Antarctic ice sheet M_{AA}.

Model projections of the sensitivity of the mass balance of the Antarctic ice sheet B_{AA} to global mean atmospheric temperature rise for the twenty-first century and are not fully compatible with the picture that emerges from the recent observations described above (Huybrechts et al., 2004; Gregory and Huybrechts, 2006). For the Antarctic ice sheet, models suggest a decrease of mass loss, or even mass gain when temperature rises because increased precipitation counteracts (or overcomes) modeled increases in ablation over the twenty-first century (Meehl et al., 2007a). The estimate of the temperature dependence of the ice

sheet mass balance from 18 AOGCMs forced with an AR4 emission scenario is $B_{AA} = -0.3\pm\ 0.2$ mm/yr/K for Antarctica with respect to local temperature changes (Meehl et al., 2007a).

However, observations display a net mass loss of the ice sheet with indications of an accelerated loss over recent years (Lemke et al., 2007). So, the sign of the sensitivity of the mass balance of Antarctica is undetermined (negative from model simulations, positive from recent observations). As for the Greenland ice sheet, recent observations have pointed out shortcomings of the ice models which raises questions on the validity of the model results. Unrepresented processes like the effects of ocean warming (Shepherd et al., 2004), ice shelf buttressing (Rignot et al., 2004; Scambos et al., 2004), and glacier ungrounding (Thomas et al., 2004) may be important. Because of this discrepancy between model results and observations, the mean sensitivity of the mass balance of the Antarctic ice sheet is set to zero in this study, and a large uncertainty is assumed: $B_{AA} = 0.0\pm\ 0.35$ mm/yr/K.

While Houghton et al. (2001) concluded that accelerated sea level rise caused by a raprid disintegration of the West Antarctic ice sheet was very unlikely in the course of the twenty-first century, Meehl et al. (2007a) acknowledge the possibility of such a rapid change based on recent changes (Shepherd et al., 2004; Vaughan, 2007). In particular, the apparent vulnerability of the glaciers in the Amundsen sector (containing an amount of ice equivalent to 1.5 m eustatic sea level rise) is emphasized by Vaughan (2007). He estimates that a mass loss equivalent to a eustatic sea level rise at a rate of 30 cm/century is not impossible in the course of the twenty-first century. Assuming a global mean temperature rise of 2 to 4 ° C over the same period yields a very rough estimate for $B_{AA,max} = 1.0$ mm/yr/K.

In the climate scenarios, the eustatic contribution of the Antarctic ice sheet is calculated in the same way as for the Greenland ice sheet (see Table III for the results). The eustatic contributions are multiplied by a factor 1.1 to account for local effects of gravity changes induced by the reduction of this land-based ice mass (see Section 5.1; Mitrovica et al., 2001, their Fig. 1a). The final contributions are listed in Table IV.

5.3.3. *Comparison to KNMI'06 and IPCC 4AR (2007)*
In van den Hurk et al. (2006), the present-day melt rate of the two ice sheets combined was estimated at $M_{AA+GL} = 0.4\pm\ 0.4$ mm/yr, based on publications available in mid-2006 (e.g., Krabill et al. (2004); Rignot and Thomas (2002); Rignot et al. (2005); Rignot and Kanagaratnam (2006); Velicogna and Wahr (2005); Zwally et al. (2005)). van den Hurk et al. (2006) used a combined estimate for the mass balance sensitivity

of the ice sheets, based mainly on recent observations, of $B_{AA+GL} = 0.2\pm 0.4$ mm/yr/K. For both the present-day melt rate and the mass balance sensitivity of the ice sheets, the values used by van den Hurk et al. (2006) are the same as the sum of the values for the individual ice sheets applied here. In van den Hurk et al. (2006), the upper bound of the contribution from the ice sheets was defined using a value for the mass balance sensitivity $B_{GL,max}$ for the Greenland ice sheet only. In light of the recent assessment of the vulnerability of the West-Antarctic Ice Sheet (Meehl et al., 2007a; Vaughan, 2007), a maximum sensitivity $B_{AA,max}$ for the Antartic ice sheet is considered here as well.

In Meehl et al. (2007a), the eustatic contribution of the Greenland and Antarctic ice sheets was based on the modeled sensitivity of the ice sheets to local temperature changes (Huybrechts et al., 2004; Gregory and Huybrechts, 2006). For the Greenland ice sheet, this eustatic contribution is 1 to 8 cm (B1, A1B and A2 scenario, Table 10.7 of Meehl et al., 2007a). For the Antarctic ice sheet, the range is -12 to -3 cm. Increased ice flow due to changing ice sheet dynamics was assessed to be more likely than reported in Houghton et al. (2001), based on new insights from observations (e.g., Alley et al., 2005; Vaughan, 2007). An estimate of 10 to 20 cm is reported, obtained by upscaling of the discharge and temperature change observed over the last decade (melt rate of $M_{GL+AA} = 0.32$ mm/yr, global mean temperature change of 0.63 ° C). The total eustatic contribution from the Greenland and Antarctic ice sheets, including this upscaled ice discharge, amounts to -5 cm to +13 cm, assuming that the central estimates reported in Table 10.7 of Meehl et al. (2007a) can be added, and their uncertainties added quadratically. The estimates presented here range from -1 cm to + 35 cm. An important difference between the two eustatic assessments arises from defining the sensitivities B and B_{max} based on observations (this study) rather than models (Meehl et al., 2007a). Although the estimates for B_{max} applied here are very uncertain, we chose to use them to estimate the contribution of the ice sheets to sea level rise. Since the impacts of sea level rise on a low-lying country like the Netherlands can be large, it is important to avoid underestimation of the contributions.

5.4. Terrestrial water storage contributions

Besides being stored in ice sheets and glaciers, water is stored on land as snow, surface waters, and subsurface water (ground water). Changes in this storage may occur due to climate variations, human interventions in the water cycle and changes in land use, for example (Church et al., 2001). Estimates of the various contributions are highly uncertain, and of different signs (Church et al., 2001; Cazenave and Nerem, 2004). The

net trend in sea level appears negative but the uncertainty bands indicate that a positive value is possible as well. In Solomon et al. (2007a), the possibility of sea level changes resulting from anthropogenic changes in terrestrial water-storage is mentioned but not quantified.

Because of the huge uncertainties involved in this contribution and to avoid underestimation of its effects, van den Hurk et al. (2006) estimated the total of the terrestrial water storage contributions to be 2 ± 2 cm in 2100 for all climate scenarios, and half of this value in 2050 (Table IV).

6. Climate scenarios of sea level rise in the northeast Atlantic Ocean

Regional climate scenarios of local sea level rise can now be constructed by combining estimates for the observed sea level rise between 1990 and 2005 (Section 3), the steric sea level rise since 2005 (Table II, Section 4), and the various changes in ocean mass (Table III, Section 5), taking into account the effects of changes in gravitation resulting from the redistribution of the mass (Section 5.1). Table IV lists all contributions of the sea level rise scenarios.

The central values can simply be added to obtain a central estimate H_c for each scenario. However, because of the large uncertainties involved in estimating all separate contributions, we present ranges of sea level rise for each atmospheric temperature scenario, rather than these single central values. The high and the low end of the range are treated separately, because of the asymmetry in the uncertainty bands of some of the contributions. The uncertainty band at each end is calculated from a quadratic summation of the uncertainty bands reported for the individual components. For the uncertainty band at the high end of the range ΔH_h, we use:

$$\Delta H_h = \sqrt{\sum_i (x_{h,i} - x_{c,i})^2} \tag{3}$$

with $x_{h,i}$ the high end of the range of contribution i, and $x_{c,i}$ the central estimate of that contribution. The summation is over all contributions i. A similar procedure is applied to define the uncertainty band at the low end of the range ΔH_l. The total range for each climate scenario becomes $(H_c - \Delta H_l, H_c + \Delta H_h)$ (Table IV).

The final figures presented to the stakeholders are rounded off to 5 cm, since the large uncertainties involved in determining the estimates do not justify a precision of one centimeter. For the moderate (warm)

climate scenario in 2050, the projected range becomes 15 cm to 25 cm (20 cm to 35 cm). For 2100, a moderate (warm) climate scenario of 30 cm to 50 cm (40 cm to 80 cm) is obtained (Table IV).

7. Summary and discussion

This paper describes the construction of climate scenarios of sea level rise for the northeast Atlantic Ocean. To arrive at these climate scenarios, information from AOGCM simulations performed in preparation of the Fourth IPCC Assessment Report, and recent observations are taken into account, as in Solomon et al. (2007a). Moreover, regional effects are incorporated, by means of the local steric sea level rise deduced from AOGCM simulations (Section 4.2) and the effect of gravity changes induced by ocean mass changes (Section 5). To our knowledge, this is the first time that gravitational effects on local sea level arising from the redistribution of mass due to melt of land-based ice masses is accounted for in climate scenarios for local sea level changes. Because of the associated gravity changes, changes in the Antarctic ice sheet are more relevant to regions in the extratropics in the northern hemispheric than changes in the Greenland ice sheet. The reverse holds for extratropical regions in southern hemisphere. For 2100, the projections for local sea level rise that are obtained range from 30 to 80 cm, depending on the rise in global mean atmospheric temperature that is assumed (Section 6).

The relation between global mean atmospheric temperature rise ΔT_{atm} and thermosteric sea level rise TS_G is assumed to be linear here (see Fig. 3). This is a simplified view of the processes involved in ocean heat uptake (Gregory et al., 2001; Raper et al., 2002). In a recent paper, Rahmstorf (2007) argues that given the large response time of the ocean on changes in atmospheric conditions, the initial rate of sea level rise is expected to be proportional to the temperature increase. That is, he stated that the relation between global mean atmospheric temperature rise ΔT_{atm} and thermosteric sea level rise TS_G is not linear, as is assumed here (see Fig. 3), but quadratic. By fitting the results of the CLIMBER 3-α model for the twentieth century, Rahmstorf (2007) found a proportionality constant for the thermosteric sea level of a=1.6 mm/yr/K. When the semi-empirical relationship outlined by Rahmstorf (2007) is used to explore future sea level rise it yields a global mean thermosteric rise of 51 cm. This is substantially larger than the central estimate of 26 cm presented by Solomon et al. (2007a). It is also 12 cm (30%) larger than the actual rise modelled by CLIMBER 3-α over the twenty-first century. A fit of

the twenty-first century data for TS_G from the six AOGCMs analyzed in this study yields a considerably smaller proportionality constant of $a = 0.9 \pm 0.03$ mm/yr/K. It is important to note, however, that the proportionality constant a is very model dependent. For the set of models analyzed here, a ranges from 0.7 mm/yr/K (MIROC3.2 (hires)) to 1.4 mm/yr/K (GISS_aom), while the individual fits are all very good (correlations larger than 0.9). Notably, all analyzed AOGCMs display a smaller proportionality constant a than the CLIMBER 3-α model analyzed by Rahmstorf (2007). As a consequence, applying the semi-empirical analysis using the ensemble mean proportionality constant $a = 0.9 \pm 0.03$ mm/yr/K yields lower estimates for TS_G than the one discussed in Rahmstorf (2007). Based on the ensemble averaged a, for the moderate (warm) scenario a central estimate for TS_G=6.3 cm (9.0 cm) in 2050 and TS_G=16.5 cm (26.5 cm) in 2100 is obtained. These numbers are very close to the applied values listed in Table II.

Because state-of-the-art AOGCMs lack reliable dynamic land ice modules and terrestrial water storage modules, information on the various components contributing to sea level rise needs to be gathered from different sources (AOGCMS, regional land ice models, recent observations), and combined in a consistent manner. Besides the fact that each of these sources has its own shortcomings, this also implies that possibly important feedbacks between the components, like for example the impacts of fresh water input due to melting land ice on the ocean circulation (Gerdes et al., 2006), are not taken into account. Such changes in the circulation will in turn affect dynamic sea level (Levermann et al., 2004). Reversely, changes in sea ice and ocean temperature will affect the local atmospheric temperature and hence land ice melt. Therefore, it is of importance to improve our understanding of the interactions between the various components of the climate system, in order to be able to reduce uncertainties in estimates for future sea level.

Acknowledgements

The authors are indebted to Roderik van der Wal and Michiel van den Broeke (IMAU, Utrecht University) for their expert comments on the contributions of melting ice masses to sea level rise in the climate scenarios. Bert Vermeersen (DEOS, Delft technical University, the Netherlands) pointed out the importance of changes in gravitation resulting from melting of land-based ice masses for local sea level changes. Douwe Dillingh (Deltares Institute, the Netherlands) provided his suggestions and comments from the stakeholders point of view during the

project. We acknowledge the modeling groups, the Program for Climate Model Diagnosis and Intercomparison (PCMDI) and the WCRP's Working Group on Coupled Modelling (WGCM) for their roles in making available the WCRP CMIP3 multi-model dataset. Support of this dataset is provided by the Office of Science, U.S. Department of Energy.

Figure captions

Figure 1:
Probability density function of global atmospheric temperature rise ΔT_{atm} for 2100 projected by available AOGCM simulations forced with A1B, A2 and B1 emission scenarios (second column in Table I). Gray shading outlines the temperature range used for the climate scenarios of sea level rise.

Figure 2:
Original versus drift-corrected data for (a) global mean thermosteric sea level rise TS_G (relative to 2005) and (b) global mean atmospheric temperature rise ΔT_{atm} (relative to 1990). Emission scenarios are distinguished by symbols (see legend), numbers are used to label the different AOGCMs

Figure 3:
Global mean thermosteric sea level rise TS_G (relative to 2005) as a function of global mean atmospheric temperature rise ΔT_{atm} (relative to 1990) for the AOGCM simulations in Table I. Gray (black) symbols denote values for 2050 (2100), solid and dashed lines outline the mean and one-standard deviation of linear fits through the data for these target years, respectively. Symbols distinguish the applied emission scenarios (see legend)

Figure 4:
Additional steric sea level rise in the eastern North Atlantic basin THS_L (relative to 2005) as a function of global mean atmospheric temperature rise ΔT_{atm} (relative to 1990) for the AOGCM simulations in Table I. Gray (black) symbols denote values for 2050 (2100), dots indicate data points at five-year intervals between these target years. Symbols distinguish the applied emission scenarios (see legend). Solid and dashed lines outline the central value and upper and lower uncertainty bounds of the contribution, respectively (see text for details on the calculation).

Figure 5:
Local steric sea level rise in the eastern North Atlantic basin THS_L

(relative to 2005) as a function of the reduction in the maximum strength of the AMOC in the Atlantic Ocean (in Sv) for the AOGCM simulations marked by an asterisk in Table I.

Figure 6:
Illustration of the effect of gravity changes on local sea level induced by a (partly) melting land-based ice mass

Table captions

Table I: Overview of AOGCM simulations (models and applied emission scenarios) used to assess the steric component of sea level rise in this study. Data for global mean thermosteric sea level rise (column marked TS_G) were available for 6 AOGCMs. Fields of local steric changes (column marked THS_L) from 10 AOGCMs were used in the analysis. Local data from the GISS models were discarded from the analysis because they contain an (unreliable) contribution from land ice melt (see Section 4). For models marked by an asterisk the relation between the meridional overturning circulation and local sea level is analyzed in Section 4.2.

Table II: Steric contributions (split between global mean thermosteric sea level change TS_G and local steric sea level change THS_L) relative to 2005, for the moderate and warm climate scenario (target years 2050 and 2100, in cm), including uncertainty ranges

Table III: Eustatic contributions from land ice (in cm) relative to 2005, for the moderate and warm climate scenario (target years 2050 and 2100), including uncertainty ranges

Table IV: Overview of all contributions incorporated in the climate scenarios (lower bound / central / upper bound). Effects of changes in gravitation are accounted for in the contributions from land ice melt (see Section 5.1, multiplication factor in parentheses)

References

Alley, R. B., P. Clark, P. huybrechts, and I. Joughin: 2005, 'Ice-sheet and sea-level changes'. *Science* **310**, 456–460.

Bahr, D. B. N., M. F. Meier, and S. D. Peckham: 1997, 'The physical basis of glacier volume-area scaling'. *J. Geophysical Res.* **102**, 20355–20362.

Bassett, S. E., M. G. A., M. J. Bentley, and P. Huybrechts: 2007, 'Modelling Antarctic sea-level data to explore the possibility of a dominant Antarctic contribution to meltwater pulse 1A'. *Quaternary Sci. Rev.* **26**, 2113–2127.

Bindoff, N., J. Willebrand, V. Artale, A. Cazenave, J. Gregory, S. Gulev, K. Hanawa, C. Le Qur, S. Levitus, Y. Nojiri, C. K. Shum, L. D. Talley, and A. Unnikrishnan: 2007, 'Observations: Oceanic Climate Change and Sea Level'. In: S. Solomon, D. Qin, M. Manning, Z. Chen, M. Marquis, K. B. Averyt, M. Tignor, and H. L. Mille (eds.): *Climate Change 2007: The Physical Science Basis. Contribution of Working Group 1 to the Fourth Assessment Report of the Intergovernmental Panel on Climate Change*. Cambridge University Press, Cambridge, United Kingdom and New York, NY, USA.

Boyer, T. P., S. Levitus, J. I. Antonov, R. A. Locarnini, and H. E. Garcia: 2005, 'Linear trends in salinity for the World Ocean, 19551998'. *Geophys. Res. Letters* **32**, L01604. doi:10.1029/2004GL021791.

Brohan, P., J. J. Kennedy, I. Haris, S. F. B. Tett, and P. D. Jones: 2006, 'Uncertainty estimates in regional and global observed temperature changes: a new dataset from 1850'. *J. Geophysical Res.* **111**, D12106.

Cazenave, A. and R. S. Nerem: 2004, 'Present-day sea-level change: observations and causes'. *Reviews of Geophysics* **42**, RG3001. doi:10.1029/2003RG000139.

Church, J. A., J. M. Gregory, P. Huybrechts, M. Kuhn, K. Lambeck, M. T. Nhuan, D. Qin, and P. L. Woodworth: 2001, 'Chapter 11. Changes in sea level'. In: J. T. Houghton et al. (ed.): *Climate Change 2001: The scientific basis. Contribution of Working Group I to the Third Assessment Report of the Intergovernmental Panel on Climate Change*. Cambridge University Press, pp. 639–693.

Church, J. A. and N. J. White: 2006, 'A twentieth century acceleration in global sea-level rise'. *Geophys. Res. Letters* **33**. doi:10.1029/2005GL02482.

Clark, P. U., J. X. Mitrovica, G. A. Milne, and M. E. Tamisiea: 2002, 'Sea-level fingerprining as a direct test for the source of global melt water pulse 1A'. *Science* **295**, 2438–2441.

Collins, W. D., C. M. Bitz, M. I. Blackmon, G. B. Bonan, C. S. Bretherton, J. A. Carton, P. Chang, S. C. Doney, J. J. Hack, T. B. Henderson, J. T. Kiehl, W. G. Large, D. S. McKenna, B. D. Santer, and R. D. Smith: 2006, 'The Community Climate System Model Version 3: CCSM3'. *J. Climate* **19**, 2122–2143–. doi: 10.1175/JCLI3761.1.

Dyurgerov, M. B. and M. F. Meier: 2005, 'Glaciers and the Changing Earth System: A 2004 Snapshot'. Occasional Paper 58, University of Colorado, Institute of Arctic and Alpine Research. Available from http://instaar.colorado.edu/other/occ_papers.htm.

Farrell, W. E. and J. A. Clark: 1976, 'On Postglacial Sea Level'. *Geophysical Journal International* **46**, 647667. doi:10.1111/j.1365-246X.1976.tb01252.x.

Flato, G. M.: 2005, 'The third generation coupled global climate model (CGCM3)'. http://www.cccma.bc.ca/modelscgcm2.shtml.

Friedlingstein, P., P. Cox, R. Betts, L. Bopp, W. von Bloh, V. Brovkin, P. Cadule, S. Doney, M. Eby, I. Fung, G. Bala, J. John, C. Jones, F. Joos, T. Kato, M. Kawamiya, W. Knorr, K. Lindsay, H. D. Matthews, T. Raddatz, P. Rayner, C. Reick, E. Roeckner, K.-G. Schnitzler, R. Schnur, K. Strassmann, A. J. Weaver, C. Yoshikawa, and N. Zeng: 2006, 'ClimateCarbon Cycle Feedback Analysis: Results from the C4MIP Model Intercomparison'. *J. Climate* **19**, 3337–3353.

Furevik, T., M. Bentsen, H. Drange, N. Kvamsto, and A. Sorteberg: 2003, 'Description and evaluation of the Bergen climate model: ARPEGE coupled with MICOM'. *Climate Dynamics* **21**, 27–51.

Gerdes, R., W. Hurlin, and S. Griffies: 2006, 'Sensitivity of a global ocean model to increased run-off from Greenland'. *Ocean Modelling* **12**, 416–435.

Gordon, C., C. Cooper, C. A. Senior, H. T. Banks, J. M. Gregory, T. C. Johns, J. F. B. Mitchell, and R. A. Wood: 2000, 'The simulation of SST, sea ice extents and ocean heat transports in a version of the Hadley Centre coupled model without flux adjustments'. *Climate Dynamics* **16**, 147–168.

Gregory, J. M., J. A. Church, G. J. Boer, K. W. Dixon, G. M. Flato, D. R. Jackett, J. A. Lowe, S. P. O'Farrell, E. Roeckner, G. L. Russell, R. J. Stouffer, and M. Winton: 2001, 'Comparison of results from several AOGCMs for global and regional sea-level change 1900-2100'. *Climate Dynamics* **18**, 241–253.

Gregory, J. M. and P. Huybrechts: 2006, 'Ice sheet contributions to future sea-level change'. *Phil. Trans. R. Soc. London A* **364**, 1709–1731. doi:10.1098/rsta.2006.1796.

Gregory, J. M. and H. Oerlemans: 1998, 'Simulated future sea-level rise due to glacier melt based on regionally and seasonally resolved temperature change'. *Nature* **391**, 474–476.

Hegerl, G. C., T. Crowley, W. Hyde, and D. Frame: 2006, 'Climate sensitivity constrained by temperature reconstructions over the past seven centuries'. *Nature* **440**, 1029–1032.

Holgate, S. J. and P. L. Woodworth: 2004, 'Evidence for enhanced coastal sea level rise during the 1990s'. *Geophys. Res. Letters* **31**, L07305.

Houghton, J. T., Y. Ding, D. J. Griggs, M. Noguer, P. J. van der Linden, X. Dai, K. Maskell, and C. A. Johnson (eds.): 2001, *Climate Change 2001: The scientific basis. Contribution of Working Group I to the Third Assessment Report of the Intergovernmental Panel on Climate Change*. Cambridge University Press. 881 pp.

Houghton, J. T., L. G. Meira Filho, B. A. Callender, N. Harris, A. Kattenberg, and K. Maskell (eds.): 1995, *Climate Change 1995: The cience of Climate Change. Contribution of Working Group 1 to the Second Assessment Report of the Intergovernmental Panel on Climate Change*. Cambridge University Press, UK.

Howat, I. M., I. Joughin, S. Tulaczyk, and S. Gogineni: 2005, 'Rapid retreat and acceleration of Helheim Glacier, east Greenland'. *Geophys. Res. Letters* **32**, L22502. doi:10.1029/2005GL024737.

Huybrechts, P., J. M. Gregory, I. Janssens, and M. Wild: 2004, 'Modelling Antarctic and Greenland volume changes during the twentieth and twenty-first centuries forced by GCM time slice integrations'. *Glob. Planet. Change* **42**, 83–105. doi:10.1016/j.gloplacha.2003.11.011.

Johannessen, O. M., K. Khvorostovsky, M. W. Miles, and L. P. Bobylev: 2005, 'Recent Ice-Sheet Growth in the Interior of Greenland'. *Science* **310**, 1013–1016. doi: 10.1126/science.1115356.

Joughin, I., W. Abdalati, and M. Fahnestock: 2004, 'Large fluctuations in speed on Greenlands Jakobshavn Isbrae glacier'. *Nature* **432**, 608–610. doi: 10.1038/nature03130.

Jungclaus, J. H., N. Keenlyside, M. Botzet, H. Haak, J. J. Luo, M. Latif, J. Marotzke, U. Mikolajewicz, and E. Roeckner: 2006, 'Ocean circulation and tropical variability in the coupled model ECHAM5/MPI-OM'. *J. Climate* **19**, 3952–3972.

K-1 model developers: 2004, 'K-1 coupled model (MIROC) description'. Technical report 1, Center for Climate System Research, University of Tokyo.

Kaser, G., J. G. Cogley, M. B. Dyurgerov, M. F. Meier, and A. Ohmura: 2006, 'Mass balance of glaciers and ice caps: consensus estimates for 1961-2004'. *Geophys. Res. Letters* **33**, L19501. doi:10129/2006GL027511.

Krabill, W., E. Hanna, P. Huybrechts, W. Abdalati, J. Cappelen, B. Csatho, E. Frederick, S. Manizade, C. Martin, J. Sonntag, R. Swift, R. Thomas, and J. Yungel: 2004, 'Greenland Ice Sheet: Increased coastal thinning'. *Geophys. Res. Letters* **31**, L24402. doi:10.1029/2004GL021533.

Lemke, P., J. Ren, R. B. Alley, I. Allison, J. Carrasco, G. Flato, Y. Fujii, G. Kaser, P. Mote, R. H. Thomas, and T. Zhang: 2007, 'Observations: Changes in Snow, Ice and Frozen Ground'. In: S. Solomon, D. Qin, M. Manning, Z. Chen, M. Marquis, K. B. Averyt, M. Tignor, and H. L. Mille (eds.): *Climate Change 2007: The Physical Science Basis. Contribution of Working Group 1 to the Fourth Assessment Report of the Intergovernmental Panel on Climate Change*. Cambridge University Press, Cambridge, United Kingdom and New York, NY, USA.

Lenderink, G., A. P. van Ulden, B. J. J. M. van den Hurk, and F. Keller: 2007, 'Climate scenarios of temperature and precipitation for the Netherlands: a study on combining global and regional climate model results'. *Climate Dynamics* **29**, 157–176.

Levermann, A., A. Griesel, M. Hofmann, M. Montoya, and S. Rahmstorf: 2004, 'Dynamic sea level changes following changes in the thermohaline circulation'. *Climate Dynamics* **24**, 347–354.

Levitus, S., J. I. Antonov, T. P. Boyer, and C. Stephens: 2000, 'Warming of the world ocean'. *Science* **287**, 2225–2229.

Lucarini, L. and G. L. Russell: 2002, 'Comparison of mean climate trends in the northern hemisphere between National Centers for Environmental Prediction and two atmosphere-ocean model forced runs'. *J. Geophysical Res.* **107 (D15)**, doi:10.1029/2001JD001247.

Meehl, G., T. F. Stocker, W. D. Collins, P. Friedlingstein, A. T. Gaye, J. M. Gregory, A. Kitoh, R. Knutti, J. M. Murphy, A. Noda, S. C. B. Raper, I. G. Watterson, A. J. Weaver, and Z.-C. Zhao: 2007a, 'Global Climate Projections'. In: S. Solomon, D. Qin, M. Manning, Z. Chen, M. Marquis, K. B. Averyt, M. Tignor, and H. L. Mille (eds.): *Climate Change 2007: The Physical Science Basis. Contribution of Working Group 1 to the Fourth Assessment Report of the Intergovernmental Panel on Climate Change*. Cambridge University Press, Cambridge, United Kingdom and New York, NY, USA.

Meehl, G. A., C. Covey, T. Delworth, M. Latif, B. McAvaney, J. F. B. Mitchell, R. J. Stouffer, and K. E. Taylor: 2007b, 'THE WCRP CMIP3 Multimodel Dataset: A New Era in Climate Change Research'. *Bull. Am. Met. Soc.* **88**, 1383–1394.

Meier, M. F.: 1984, 'Contribution of small glaciers to global sea level'. *Science* **226**, 1418–1421.

Meier, M. F., M. B. Dyurgerov, U. K. Rick, S. O'Neel, W. T. Pfeffer, R. S. Anderson, S. P. Anderson, and A. F. Glazovsky: 2007, 'Glaciers dominate eustatic sea-level ris ein the 21st century'. *Science* **317**, 1064–1067. doi:10.1126/science.1143906.

Mitrovica, J. X., M. E. Tamisiea, J. L. Davis, and G. A. Milne: 2001, 'Recent mass balance of polar ice sheets inferred from patterns of global sea level change'. *Nature* **409**, 1026–1029.

Ohmura, A.: 2004, 'Cryosphere during the Twentieth Century, The State of the Plane'. *IUGG Geophys. Monograph* **150**, 239–257.

Oppenheimer, M.: 1998, 'Global warming and the stability of the West Antarctic Ice Sheet'. *Nature* **393**, 325–332.

Otto-Bliesner, B. L., S. J. Marshall, O. J. T., G. H. Miller, A. Hu, and CAPE Last Interglaciation Project members: 2006, 'Simulating Arctic climate warmth and ice-field retreat in the last interglaciation'. *Science* **311**, 1751–1753. doi:10.1126/science.1120808.

Rahmstorf, S.: 2007, 'A semi-empirical approach to projecting future sea level rise'. *Science* **315**, 368 – 370. doi:10.1126/science.1135456.

Raper, S. C. B. and R. J. Braithwaite: 2006, 'Low sea level rise projections from mountain glaciers and icecaps under global warming'. *Nature* **439**, 311–31.

Raper, S. C. B., J. M. Gregory, and R. J. Stouffer: 2002, 'The role of climate sensitivity and ocean heat uptake on AOGCM transient temperature response'. *J. Climate* **15**, 124–130.

Rayner, N. A., P. Brohan, D. E. Parker, C. K. Folland, J. J. Kennedy, M. Vanicek, T. Ansell, and S. F. B. Tett: 2006, 'Improved analyses of changes and uncertainties in marine temperature measured in situ since the mid-nineteenth century: the HadSST2 dataset'. *J. Climate* **19**, 446–469.

Ridley, J. K., P. Huybrechts, J. M. Gregory, and J. A. Lowe: 2005, 'Elimination of the Greenland ice sheet in a high CO_2 climate'. *J. Climate* **17**, 3409–3427.

Rignot, E., G. Casassa, P. Gogineni, W. Krabill, A. Rivera, and R. Thomas: 2004, 'Accelerated ice discharge from the Antarctic Peninsula following the collapse of Larsen B ice shelf'. *Geophys. Res. Letters* **31**, L18401. doi:10.1029/2004GL020697.

Rignot, E. G., G. Casassa, P. Gogineni, P. Kanagaratman, W. Krabill, H. Pritchard, A. Rivera, R. Thomas, J. Turner, and D. Vaughan: 2005, 'Recent ice loss from the Fleming and other glaciers, Wordie Bay, West Antarctic Peninsula'. *Geophys. Res. Letters* **32**, 1–4.

Rignot, E. G. and P. Kanagaratnam: 2006, 'Changes in the Velocity Structure of the Greenland Ice Sheet'. *Science* **311**, 986–990.

Rignot, E. G. and R. H. Thomas: 2002, 'Mass balance of polar ice sheets'. *Science* **297**, 1502–1506.

Scambos, T., J. A. Bohlander, C. A. Shuman, and P. Skvarca: 2004, 'Glacier acceleration and thinning after ice shelf collapse in the Larsen B embayment, Antarctica'. *Geophys. Res. Letters* **31**, L18402. doi:10.1029/2004GL020670.

Schmidt, G. A., R. Ruedy, J. E. Hansen, I. Aleinov, N. Bell, M. Bauer, S. Bauer, B. Cairns, V. Canuto, Y. Cheng, A. Del Genio, G. Faluvegi, A. D. Friend, T. M. Hall, Y. Hu, M. Kelley, N. Y. Kiang, D. Koch, A. A. Lacis, J. Lerner, K. K. Lo, R. L. Miller, L. Nazarenko, V. Oinas, J. Perlwitz, D. Rind, A. Romanou, G. L. Russell, M. Sato, D. T. Shindell, P. H. Stone, S. Sun, N. Tausnev, D. Thresher, and M. S. Yao: 2004, 'Present day atmospheric simulations using GISS ModelE: Comparison to in-situ, satellite and reanalysis data'. *J. Climate* **19**, 153–192.

Schmittner, A., M. Latif, and B. Schneider: 2005, 'Model projections of the North Atlanioc thermohaline circulation for the 21st century assessed by observations'. *Geophys. Res. Letters* **32**, L23710.

Shepherd, A. and D. Wingham: 2007, 'Recent sea-level contributions of the Antractic and Greenland ice sheets'. *Science* **315**, 1529–1532.

Shepherd, A., D. Wingham, and E. Rignot: 2004, 'Warm ocean is eroding West Antarctic Ice Sheet'. *Geophys. Res. Letters* **31**, L23402. doi:10.1029/2004GL02110.

Solomon, S., D. Qin, M. Manning, Z. Chen, M. Marquis, K. B. Averyt, M. Tignor, and H. L. Mille (eds.): 2007a, *Climate Change 2007: The Physical Science Basis. Contribution of Working Group 1 to the Fourth Assessment Report of*

the Intergovernmental Panel on Climate Change. Cambridge University Press, Cambridge, United Kingdom and New York, NY, USA.

Solomon, S., D. Qin, M. Manning, Z. Chen, M. Marquis, K. B. Averyt, M. Tignor, and H. L. Mille: 2007b, 'Summary for Policymakers'. In: *IPCC , 2007: Climate Change 2007: The Physical Science Basis. Contribution of Working Group 1 to the Fourth Assessment Report of the Intergovernmental Panel on Climate Change*. Cambridge University Press, Cambridge, United Kingdom and New York, NY, USA.

Stainforth, D. A., T. Aina, C. Christensen, M. Collins, N. Faull, D. J. Frame, J. A. Kettleborough, S. Knight, A. Martin, J. M. Murphy, C. Piani, D. Sexton, L. A. Smith, R. A. Spicer, A. Thorpe, and M. R. Allen: 2005, 'Uncertainty in predictions of the climate response to rising levels of greenhouse gases'. *Nature* **433**, 403–406.

Thomas, R., E. Rignot, G. Casassa, P. Kanagaratnam, C. Acuna, T. Akins, H. Brecher, E. Frederick, P. Gogineni, W. Krabil, S. Manizade, H. Ramamoorthy, A. Rivera, R. Russell, J. Sonntag, R. Swift, J. Yungel, and J. Zwally: 2004, 'Accelerated Sea-Level Rise from West Antarctica'. *Science* **306**, 255–258. DOI: 10.1126/science.1099650.

van de Wal, R. S. W. and M. Wild: 2001, 'Modelling the response of glaciers to climate change, applying volume-area scaling in combination with a high resolution GCM'. *Climate Dynamics* **18**, 359–366.

van den Hurk, B. J. J. M., A. M. G. Klein Tank, G. Lenderink, A. P. van Ulden, G. J. van Oldenborgh, C. A. Katsman, H. W. van den Brink, F. Keller, J. J. F. Bessembinder, G. Burgers, G. J. Komen, W. Hazeleger, and S. S. Drijfhout: 2006, 'KNMI Climate Change Scenarios 2006 for the Netherlands'. Technical report WR-2006-01, KNMI. Available from www.knmi.nl/climatescenarios.

van der Schrier, G., S. L. Weber, and S. S. Drijfhout: 2004, 'Low-frequency sea-level variability in the Atlantic'. *Glob Plan Change* **43**, 129–1442.

van Ulden, A. P. and G. J. van Oldenborgh: 2006, 'Global climatic impacts of a collapse of the Atlantic thermohaline circulation'. *Atm Chem Phys* **6**, 863–881.

Vaughan, D. G.: 2007, 'West Antarctic Ice Sheet collapse - the fall and rise of a paradigm'. *Climatic Change*. in press.

Velicogna, I. and J. Wahr: 2005, 'Greenland mass balance from GRACE'. *Geophys. Res. Letters* **32**, L18505.

Vellinga, M. and R. A. Wood: 2002, 'Global climatic impacts of a collapse of the Atlantic thermohaline circulation'. *Climatic Change* **54**, 251–267.

Volodin, E. M. and N. A. Diansky: 2004, 'El-Niño reproduction in coupled general circulation model of atmosphere and ocean'. *Russian meteorology and hydrology* **12**, 5–14.

Washington, W. M., J. W. Weatherly, G. A. Meehl, A. J. Semtner Jr, T. Bettge, A. Craig, W. Strand Jr, J. Arblaster, V. Wayland, R. James, and Y. Zhang: 2000, 'Parallel climate model (PCM) control and transient simulations'. *Climate Dynamics* **16**, 755–774.

Wigley, T. M. L. and S. C. B. Raper: 2005, 'Extended scenarios for glacier melt due to anthropogenic forcing'. *Geophys. Res. Letters* **32**, L05704. doi: 10.1029/2004GL021238.

Woodward, R. S.: 1888, 'On the form and position of mean sea level'. *US Geol. Surv. Bull.* **48**, 87–170.

Yu, Y., X. Zhang, and Y. Guo: 2004, 'Global coupled ocean- atmosphere general circulation models in LASG/IAP'. *Adv. Atmos. Sci* **21**, 444–455.

Yukimoto, S. and A. Noda: 202, 'Improvements of the Meteorological Research Institute Global Ocean-atmosphere Coupled GCM (MRI-CGCM2) and its climate sensitivity'. Technical report 10, NIES, Japan.

Zwally, H., M. Giovinetto, J. Li, H. Cornejo, M. Beckley, A. Brenner, and co-authors: 2005, 'Mass changes of the Greenland and Antarctic ice sheets and shelves and contributions to sea level rise: 1992-2002'. *J. Glac.* **51**, 509–527.

Tables

Table I. Overview of AOGCM simulations (models and applied emission scenarios) used to assess the steric component of sea level rise in this study. Data for global mean thermosteric sea level rise (column marked TS_G) were available for 6 AOGCMs. Fields of local steric changes (column marked THS_L) from 10 AOGCMs were used in the analysis. Local data from the GISS models were discarded from the analysis because they contain an (unreliable) contribution from land ice melt (see Section 4). For models marked by an asterisk the relation between the meridional overturning circulation and local sea level is analyzed in Section 4.2.

	TS_G	THS_L	reference
BCCR-BCM2.0*		B1, A2	Furevik et al. (2003)
CCSM3.0		B1, A1B, A2	Collins et al. (2006)
CGCM3.1 (T47)*	B1, A1B, A2	B1, A1B, A2	Flato (2005)
ECHAM5/MPI-OM*		B1, A1B, A2	Jungclaus et al. (2006)
FGOALS-g1.0*		B1, A1B	Yu et al. (2004)
GISS-AOM	B1, A1B	[discarded]	Lucarini and Russell (2002)
GISS-ER	B1, A1B, A2	[discarded]	Schmidt et al. (2004)
INM-CM3.0	B1, A1B, A2		Volodin and Diansky (2004)
MIROC3.2 (hires)*	B1, A1B	B1, A1B	K-1 model developers (2004)
MIROC3.2 (medres)*	B1, A1B, A2	B1, A1B, A2	K-1 model developers (2004)
MRI-CGCM2.3.2*		B1, A1B, A2	Yukimoto and Noda (202)
PCM		A2	Washington et al. (2000)
UKMO_HadCM3		B1, A1B, A2	Gordon et al. (2000)

Table II. Steric contributions (split between global mean thermosteric sea level change TS_G and local steric sea level change THS_L) relative to 2005, for the moderate and warm climate scenario (target years 2050 and 2100, in cm), including uncertainty ranges

	moderate		warm	
year (ΔT_{atm} since 1990)	2050 (1° C)	2100 (2° C)	2050 (2° C)	2100 (4° C)
TS_G **(cm)**				
central	6.9	20.1	11.3	29.8
lower bound	4.5	15.6	8.9	25.3
upper bound	9.3	24.6	13.7	34.3
THS_L **(cm)**				
central	0.8	1.6	1.6	3.1
lower bound	-0.8	-1.7	-1.7	-3.3
upper bound	4.2	8.4	8.4	16.7

Table III. Eustatic contributions from land ice (in cm) relative to 2005, for the moderate and warm climate scenario (target years 2050 and 2100), including uncertainty ranges

	moderate		warm	
year (ΔT_{atm} since 1990)	2050 (1° C)	2100 (2° C)	2050 (2° C)	2100 (4° C)
glaciers (cm)				
central	4.5	10.7	6.0	14.5
lower bound	3.5	8.1	4.7	10.1
upper bound	5.6	13.6	7.5	19.3
Greenland (cm)				
central	1.2	3.5	1.7	5.4
lower bound	0.7	1.7	0.8	2.3
upper bound	3.3	13.1	6.2	25.4
Antarctica (cm)				
central	0.9	1.9	0.9	1.9
lower bound	-0.9	-3.1	-1.5	-6.2
upper bound	3.5	11.9	5.7	21.4

Table IV. Overview of all contributions incorporated in the climate scenarios (lower bound / central / upper bound, in cm). Effects of changes in gravitation are accounted for in the contributions from land ice melt (see Section 5.1, multiplication factor in parentheses)

	moderate		warm	
year (ΔT_{atm} since 1990)	2050 (1° C)	2100 (2° C)	2050 (2° C)	2100 (4° C)
observed 1990-2005	3.0/4.0/5.0	3.0/4.0/5.0	3.0/4.0/5.0	3.0/4.0/5.0
steric rise since 2005	4.8/7.7/11.9	16.1/21.7/29.9	8.8/12.9/20.1	25.1/32.9/47.2
glaciers (0.8)	2.8/3.6/4.5	6.5/8.6/10.9	3.8/4.8/6.0	8.1/11.6/15.4
Greenland (0.25)	0.2/0.3/0.8	0.4/0.9/3.3	0.2/0.4/1.5	0.6/1.4/6.4
Antarctica (1.1)	-0.9/1.0/3.9	-3.4/2.1/13.1	-1.6/1.0/6.2	-6.8/2.1/23.5
terrestrial water storage	0.0/1.0/2.0	0.0/1.0/2.0	0.0/1.0/2.0	0.0/1.0/2.0
total	13.8/17.6/22.9	30.0/38.2/52.4	19.0/24.1/33.3	40.5/53.0/79.5
total, rounded off range	15 / 25	30 / 50	20 / 35	40 / 80

Figures

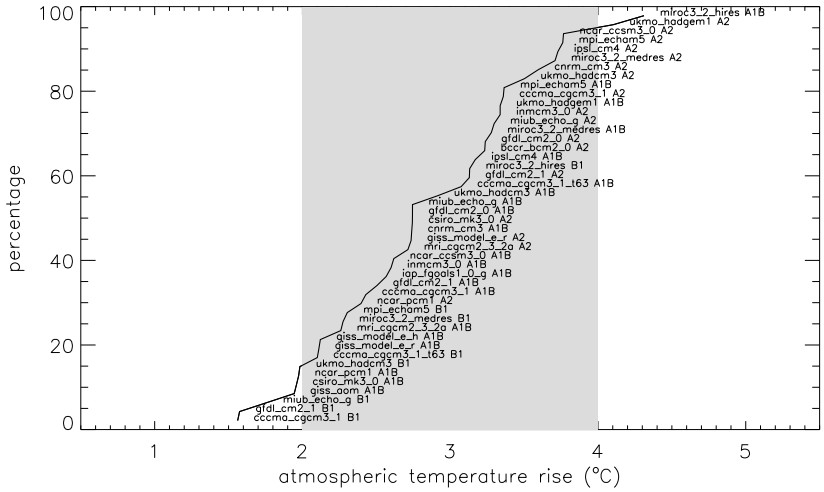

Figure 1. Probability density function of global atmospheric temperature rise ΔT_{atm} for 2100 projected by available AOGCM simulations forced with A1B, A2 and B1 emission scenarios (second column in Table I). Gray shading outlines the temperature range used for the climate scenarios of sea level rise.

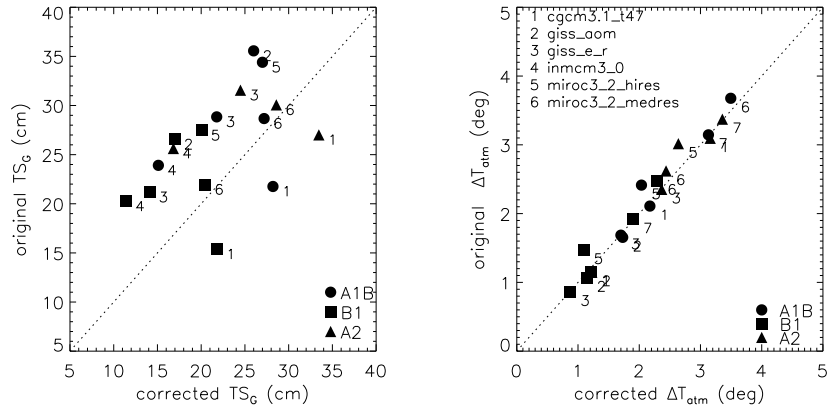

Figure 2. Original versus drift-corrected data for (a) global mean thermosteric sea level rise TS_G (relative to 2005) and (b) global mean atmospheric temperature rise ΔT_{atm} (relative to 1990). Emission scenarios are distinguished by symbols (see legend), numbers are used to label the different AOGCMs

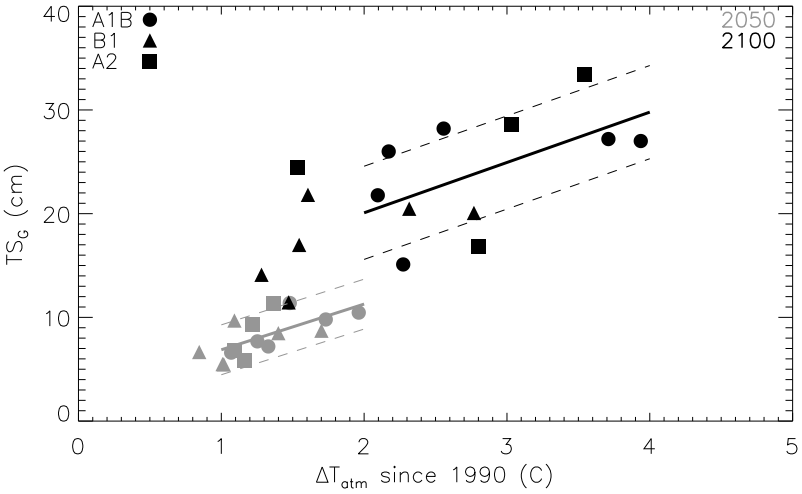

Figure 3. Global mean thermosteric sea level rise TS_G (relative to 2005) as a function of global mean atmospheric temperature rise ΔT_{atm} (relative to 1990) for the AOGCM simulations in Table I. (ΔT_{atm} relative to 1990 = ΔT_{atm} relative to 2005 + 0.27° C). Gray (black) symbols denote values for 2050 (2100), solid and dashed lines outline the mean and one-standard deviation of linear fits through the data for these target years, respectively. Symbols distinguish the applied emission scenarios (see legend)

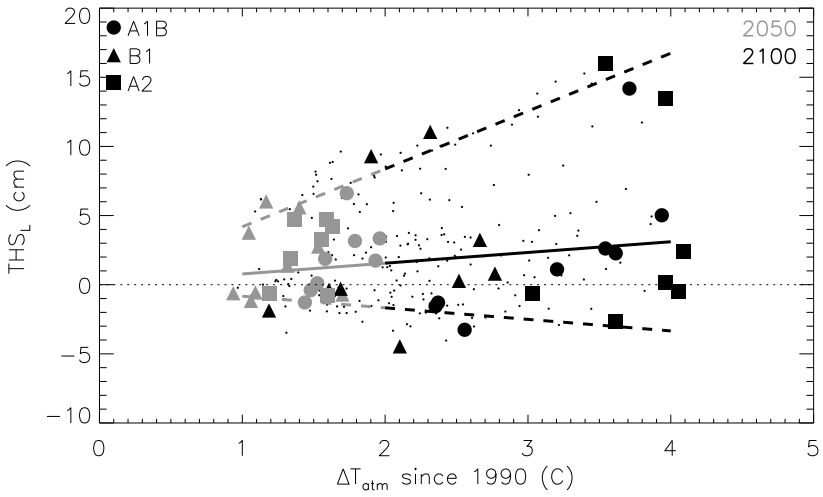

Figure 4. Additional steric sea level rise in the eastern North Atlantic basin THS_L (relative to 2005) as a function of global mean atmospheric temperature rise ΔT_{atm} (relative to 1990) for the AOGCM simulations in Table I (ΔT_{atm} relative to 1990 = ΔT_{atm} relative to 2005 + 0.27° C). Gray (black) symbols denote values for 2050 (2100), dots indicate data points at five-year intervals between these target years. Symbols distinguish the applied emission scenarios (see legend). Solid and dashed lines outline the central value and upper and lower uncertainty bounds of the contribution, respectively (see text for details on the calculation).

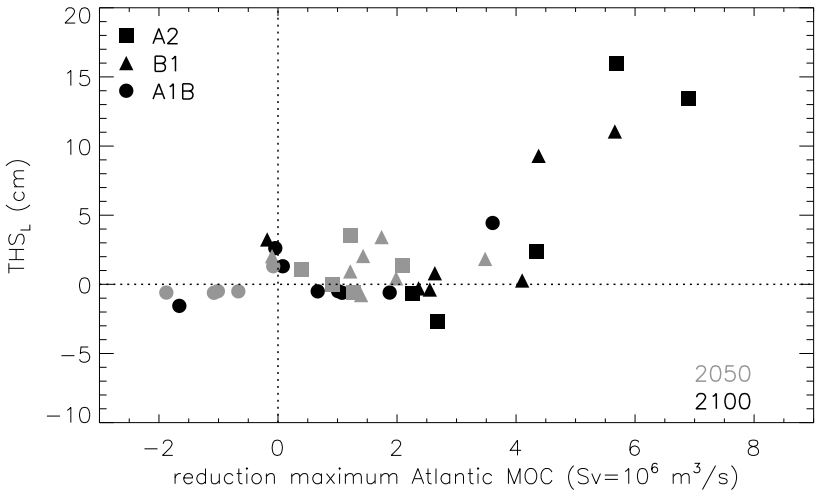

Figure 5. Local steric sea level rise in the eastern North Atlantic basin THS_L (relative to 2005) as a function of the reduction in the maximum strength of the AMOC in the Atlantic Ocean (in Sv) for the AOGCM simulations marked by an asterisk in Table I.

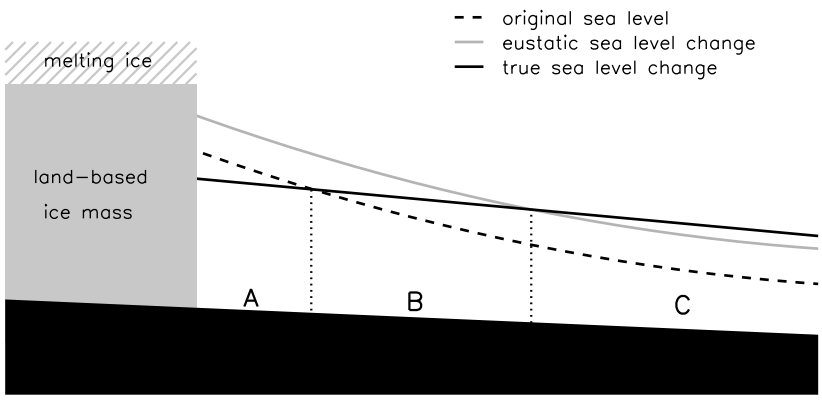

Figure 6. Illustration of the effect of gravity changes on local sea level induced by a (partly) melting land-based ice mass